Effects of monolayer AlAs insertion in modulation doped GaAs/$Al_xGa_{1-x}As$ quantum-well structures

Q. X. Zhao,[1] S. Wongmanerod,[2] M. Willander,[1] P. O. Holtz,[2] E. Selvig[3] and B. O. Fimland,[3]
[1]*Physical Electronics and Photonics, Department of Microelectronics and Nanoscience, Chalmers University of Technology and Göteborg University, S-412 96 Göteborg, Sweden*
[2]*Department of Physics, Linköping University of Technology, S-583 81 Linköping, Sweden*
[3]*Department of Physical Electronics, Norwegian University of Science and Technology, N-7034 Trondheim, Norway*
(Received 24 April 2000)

Symmetrically modulation doped GaAs/$Al_xGa_{1-x}As$ quantum-well structures, containing a monolayer thickness of single AlAs insertion in the well region, are studied by photoluminescence spectroscopy and electrical characterization. The aim of this study is to explore how the AlAs insertion influences the electronic properties of the structures and the mobility of the carrier confined in the well layer. We find that the electronic structure of the confined electrons is strongly influenced by the AlAs insertion in the modulation doped structures. The effective mass of the particles involved in the observed optical transition and the transition energy were deduced from magneto-optical measurements, while the mobility and carrier concentration were obtained from the Hall measurements. The experimentally deduced transition energies are compared with the results from a simple self-consistent calculation.

INTRODUCTION

Modulation doped GaAs/$Al_xGa_{1-x}As$ structures have been subject to extensive investigations during the past two decades. The experimental results provide a comprehensive understanding of the optical and electrical properties of the structures. Radiative recombination related to the two-dimensional electron gas and many-body effects such as the Fermi-edge singularity (FES) have been observed in modulation doped GaAs/$Al_xGa_{1-x}As$ heterostructures[1–6] and $In_xGa_{1-x}As$/InP quantum-well (QW) structures.[7,8] It is also well known that the carrier mobility in modulation doped heterostructures is strongly enhanced in comparison with bulk materials due to a reduction of the impurity scattering.[9] To the best of our knowledge, there are much fewer studies of modulation doped GaAs/$Al_xGa_{1-x}As$ QW structures containing an AlAs insertion in the well region, although there are many reports on the undoped monolayer structures in the GaAs/$In_xGa_{1-x}As$ (Refs. 10 and 11) and CdTe/ZnTe systems.[12,13] In addition, our study also intends to verify the theoretical prediction on the variation of the carrier mobility due to the change of the electron-phonon interaction in GaAs/$Al_xGa_{1-x}As$ QW's with a monolayer insertion.[14,15] According to the theoretical calculations, the carrier mobility strongly depends on the position of inserted AlAs layer in modulation doped GaAs/AlAs/$Al_xGa_{1-x}As$ QW structures.

In this investigation, *n*-type symmetrically modulation doped GaAs/$Al_xGa_{1-x}As$ quantum-well structures are used. An AlAs layer with a two-monolayer thickness is placed at different positions in the well region. The structures are characterized by magneto-optical spectroscopy and Hall measurements. We find that the electronic structure of the confined electrons is strongly influenced by the inserted AlAs layer in the modulation doped structures. The effective mass of the particles involved in the observed optical transition and the transition energy were deduced from magneto-optical measurements, while the mobility and carrier concentration were obtained from the Hall measurements. The experimentally deduced transition energies are compared with the results from a simple self-consistent calculation.

SAMPLES AND EXPERIMENT

The samples used in this study are grown by molecular-beam epitaxy (MBE). The reference sample As375 is a symmetric modulation doped 150 Å GaAs/$Al_{0.3}Ga_{0.7}As$ quantum well. There is a 100 Å $Al_{0.3}Ga_{0.7}As$ spacer layer on both sides of the GaAs well layer. The doping region is a 100-Å-wide $Al_{0.3}Ga_{0.7}As$ barrier layer with a Si doping concentration of $1\times10^{18}\,cm^3$. Sample As364 and sample As374 have the same structure design as the reference sample As375, except there is an AlAs insertion layer with two monolayer thickness in the 150 Å GaAs well layer at a position of 50 and 75 Å, respectively, from the top interface. In order to vary the carrier concentration but keeping the other structure parameters unchanged, atomic hydrogen was introduced into the samples by a dc-plasma technique.[16] The three as-grown samples were treated at the same time by dc hydrogen plasma at 250 °C for half an hour. The hydrogen treated samples are denoted as As375H, As364H, and As374H, respectively. During the hydrogen treatment, the samples were mounted on a heater block, with which the sample temperature can be controlled with a ±2 °C accuracy, and placed 10 cm downstream from the plasma with a bias voltage of 300 V. The pressure of the plasma was 1.5 mbar. The hydrogen treatment will not affect the structure quality of the samples at the above conditions.[16]

A double grating monochromator and a photomultiplier were used to disperse and detect the photoluminescence (PL) and PL excitation (PLE) signals. For zero magnetic field PL measurements, an Oxford Variox variable temperature cryostat was used. The sample temperature could be continuously regulated down to 1.5 K. An Ar^+ laser and an Ar^+ laser

 ©2000 The American Physical Society

TABLE I. Mobility (μ), carrier concentration (n), and effective mass (m^*_{eff}) obtained from as-grown samples As375, As364, and As374, as well as from H-passivated samples As375H, As364H, and As374H.

	As375	As364	As374	As375H	As364H	As374H
Position of the inserted AlAs layer relative to top interface	0 as-grown	50 Å as-grown	75 Å as-grown	0 H-treated	50 Å H-treated	75 Å H-treated
μ (cm^2/V s) at 10 K	3.1×10^4	3.0×10^4	2.9×10^4	2.4×10^4	2.2×10^4	2.9×10^4
n (1/cm^2) at 10 K	1.45×10^{12}	1.20×10^{12}	1.23×10^{12}	0.72×10^{12}	0.54×10^{12}	0.59×10^{12}
μ (cm^2/V s) at 160 K	1.7×10^4	1.6×10^4	1.4×10^4	1.3×10^4	1.3×10^4	1.5×10^4
n (1/cm^2) at 160 K	1.90×10^{12}	1.60×10^{12}	1.76×10^{12}	1.23×10^{12}	0.84×10^{12}	0.98×10^{12}
μ (cm^2/V s) at 294 K	7.1×10^3	6.8×10^3	6.3×10^3	6.4×10^3	5.8×10^3	6.5×10^3
n (1/cm^2) at 294 K	2.20×10^{12}	1.85×10^{12}	2.09×10^{12}	1.49×10^{12}	0.94×10^{12}	1.11×10^{12}
m^*_{eff} (ehh11)	0.070	0.060	0.060	0.066	0.066	0.066
m^*_{eff} (ehh21)	0.053	0.055	0.060			

pumped tunable sapphire: Ti solid-state laser were used as the excitation sources. The magneto-optical measurements were carried out in a 14 T magnet in the Faraday configuration. The laser was coupled to the sample via optical fibers, and the emissions from the sample were collected through the same fiber into the monochromator.

RESULTS AND DISCUSSIONS

From the Hall measurements, the mobility and carrier concentration in each sample were deduced. The results are summarized in Table I at room temperature, 160 K, and 10 K. The results clearly indicate that the carrier density in the well decreases in the hydrogen-treated samples in comparison with the corresponding as-grown samples. The reduction of the carrier concentration is about 50%. The high-resolution x-ray defraction measurements were used to characterize the as-grown samples and the H-treated samples. The results indicate that the quality of the structures remains unchanged after the passivation, which is consistent with earlier conclusions for QW structures after the same H-treatment conditions.[16]

The as-grown and the H-treated samples were characterized by PL measurements. Figure 1(a) shows the PL spectra from the three as-grown samples, measured at 2.0 K with an excitation wavelength of 5145 Å from an Ar^+ laser. The radiative recombination related to the two-dimensional electron gas (2DEG) appears at an energy higher than the energy of the bulk GaAs excitons. The two peaks are explained in terms of recombination from two electron subbands. This interpretation will be further expounded upon below. The significant difference concerning the transition energy, PL line shape, and relative PL intensity of the 2DEG transitions are illustrated in the figure for the three different samples. It clearly shows that the transition energy shifts to higher en-

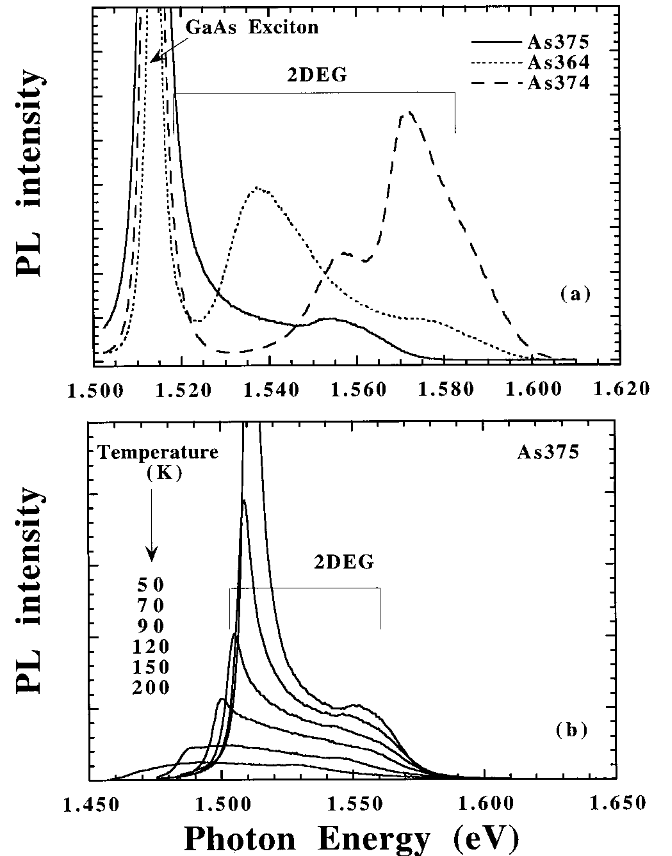

FIG. 1. (a) PL spectra from the three as-grown samples (As375, As364, and As374), measured at 2.0 K. The excitation power is 4 mW and the excitation wavelength is 5145 Å from an Ar^+ laser. (b) Temperature dependence of the PL from sample As375. The excitation conditions are (a).

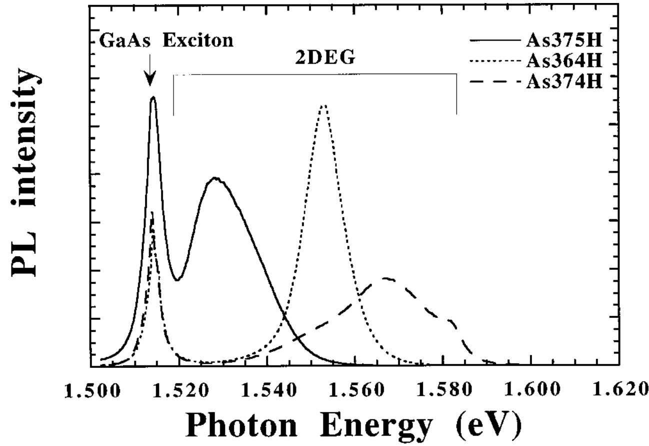

FIG. 2. PL spectra from the three H-passivated samples (As375H, As364H, and As374H), measured at 2.0 K. Excitation power is 4 mW and excitation wavelength is 5145 Å from an Ar^+ laser.

ergy when the AlAs inserted layer is placed close to the center of the well. The low-energy side of the 2DEG transition from sample As375 is overlapping with the bulk GaAs excitons, which is illustrated in Fig. 1(b) at different temperatures. This will be further illustrated by the magneto-optical data, which will be presented below. Figure 2 illustrates the PL spectra for the hydrogen-treated samples at the same excitation conditions as shown in Fig. 1. In comparison with the as-grown samples shown in Fig. 1(a), the results clearly show that the 2DEG concentration decreases, which is consistent with the results of the Hall measurements. Furthermore, the PL spectra also indicate that the energy position of the 2DEG related transitions shifts towards higher energy after the H treatment. Furthermore, only one occupied electron subband transition was observed for the three samples after the H treatments.

In order to accurately determine the 2DEG transition energies, we have performed the PL measurements and PL excitation (PLE) measurements under different applied magnetic fields along the growth direction. A typical group of PL and PLE spectra are shown in Figs. 3 and 4, obtained from the as-grown sample As364 and H-treated sample As364H at different magnetic fields. The Landau-level splitting is clearly seen both in the PL and the PLE spectra. By comparing Figs. 3(b) and 4(b), it is obvious that the electron concentration in sample As364H is much lower than in As364. The Fermi energy is about 43 meV above the ground state with two occupied electron subbands in as-grown sample As364, while the Fermi energy is about 21 meV above the ground state with only one occupied electron subband in sample As364H. Taking into account that the second electron level is only slightly populated in As364, the roughly estimated Fermi energy is consistent with the reduction of the electron concentration by about 50% after the H treatment. A typical diagram of the transition energies from magneto-optical measurements for the as-grown sample As375 is illustrated in Fig. 5, where the filled circles represent data from the PL measurements and open circles from the PLE measurements. The lines in the figure are calculated by using the following expression:

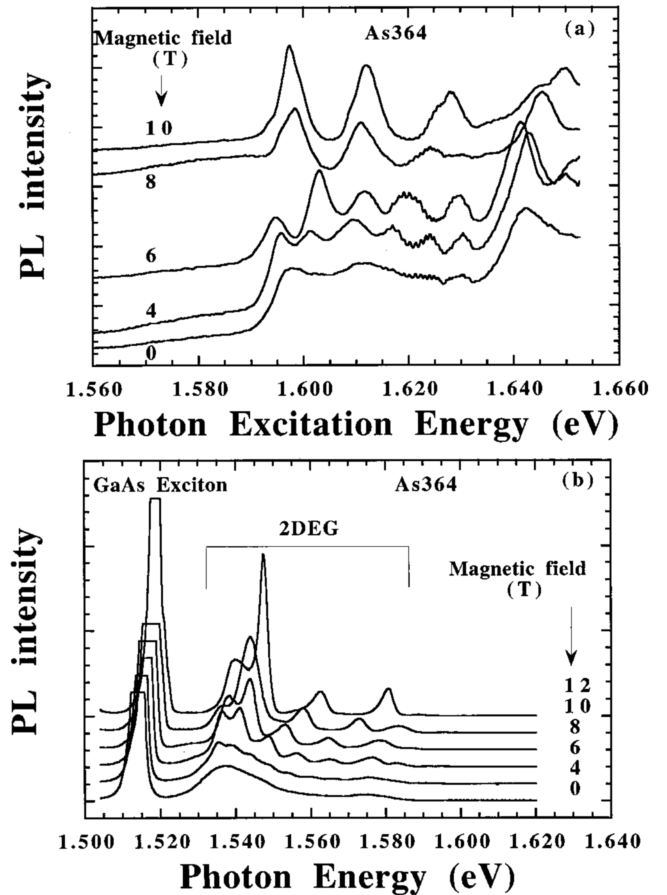

FIG. 3. (a) PLE spectra from sample As364, measured at different magnetic fields. (b) PL spectra from sample As364, measured at different magnetic fields.

$$E(B)=E(0)+(n+\tfrac{1}{2})\hbar\omega_c=E(0)+(n+\tfrac{1}{2})\frac{\hbar eB}{m^*}, \quad (1)$$

where $E(0)$ is the energy separation between the corresponding electron and hole subbands involved in the recombination at zero magnetic field. m^* is the effective mass of the involved electron and hole, $1/m^*=(1/m_e^*)+(1/m_h^*)$, and B is the magnetic-field strength. The effective mass m^* is a fitting parameter. Similar measurements and fitting procedures were applied to the other samples, and the results of the deduced effective mass are listed in Table I, and deduced zero field energies are summarized in Fig. 7 as circles.

To confirm or reject the interpretation of the two PL transition bands observed in the as-grown samples as being due to the emission from two different electron subbands, we have performed a self-consistent calculation. The confined electron and hole levels in the structures are obtained. The details of the theoretical calculations and the parameters used in the calculations, the reader is referred to Refs. 2 and 13. Once these electron and hole Schrödinger equations have been solved, the optical transition energies can be calculated. The calculated potential and wave functions for the first two subbands are shown in Fig. 6 for the as-grown samples. The calculated results may be affected by the band-gap renormalization,[17–19] since the electron density is rather high in our structures. However, the band-gap renormalization energy will be very similar in all as-grown structures investi-

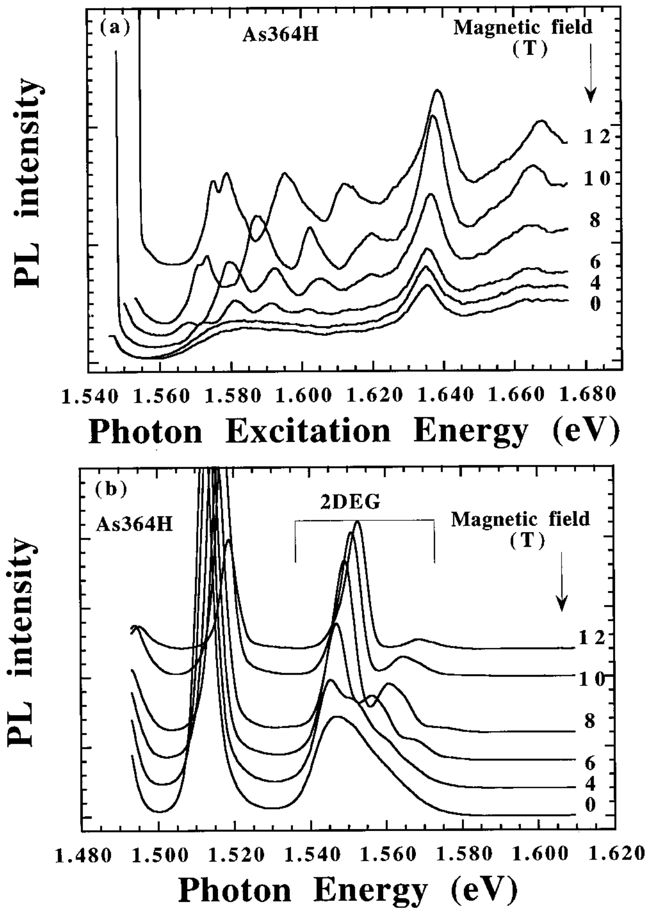

FIG. 4. (a) PLE spectra from sample As364H, measured at different magnetic fields. (b) PL spectra from sample As364H, measured at different magnetic fields.

gated here, since they have a similar electron density. Therefore, in this first approximation we have not included such effects, since the purpose of this calculation is just to provide guidance for the interpretation of the observed transitions. Instead, when we compare the calculated and experimental results, we downshift the same energy for all structures studied here. There could be some difference between the as-

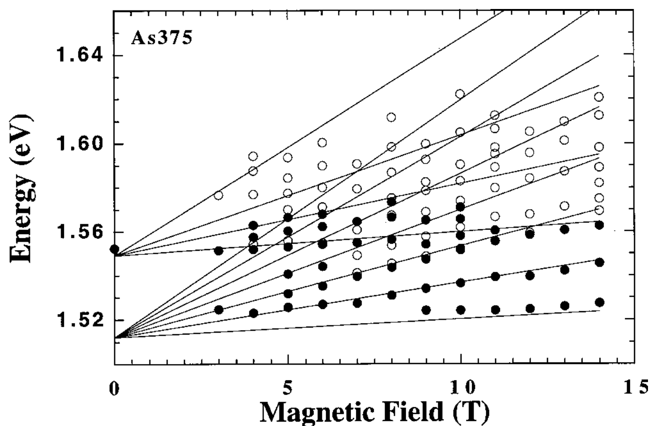

FIG. 5. Landau-level splitting for sample As375. The circles correspond to our experimental results (open and filled circles are from PLE and PL measurements, respectively), while the lines show the calculated Landau-level position according to Eq. (1).

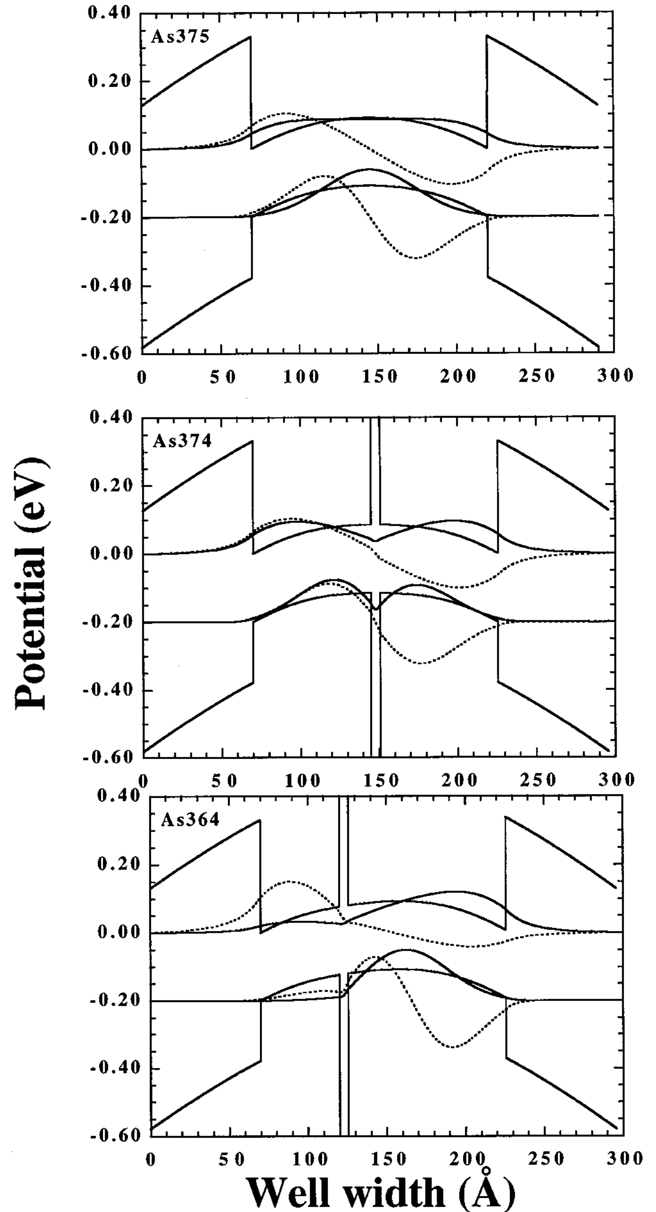

FIG. 6. The electron and hole potentials and the calculated first two subband wave functions. The solid line represents the first subband, and dotted line represents the second subband.

grown and the H-treated structures, but such a difference will not mislead the interpretation of the results. The calculated results are shown in Fig. 7 as solid lines for the as-grown samples and dotted lines for the H-treated samples. The electron concentrations deduced from the Hall measurements were used in the calculations. The calculated transitions were downshifted 13 meV for all transitions and all structures. The good agreement in the tendency indicates that the first transition observed in all structures is related to the first electron level and the first heavy-hole level in the structures, denoted as ehh11, while the second transition is related to the second electron level and the first heavy-hole level, denoted as ehh21, except sample As374, in which the transition energies for ehh22, elh11, and ehh21 are very close. Taking into account the much larger oscillator strength for the transition ehh22 and the deduced similar effective mass as the transition ehh11, the observed second transition in sample

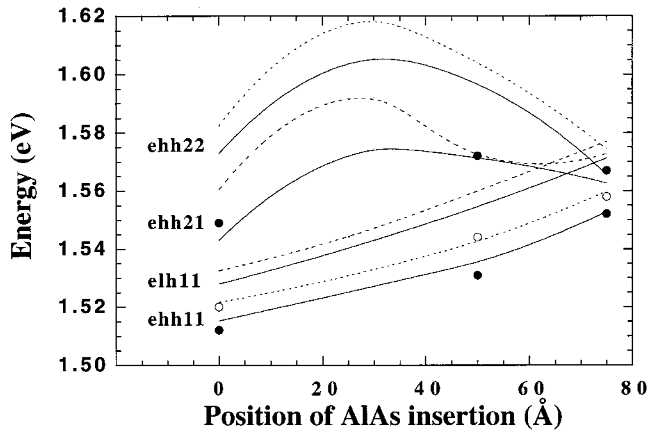

FIG. 7. Circles represent the experimentally deduced 2DEG emission energies. Filled circles are from the as-grown samples, and open circles represent the results from the H-passivated samples. The solid lines and dotted lines are calculated results for the as-grown and the H-passivated samples, respectively.

As374 is most likely related to the hh22 transition, i.e., the second electron subband and the second heavy-hole subband. This assignment is consistent with the relative PL intensity observed in Fig. 1. In symmetric QW structures, the transition ehh21 is forbidden according to the dipole selection rule. Such a dipole selection rule may be relaxed to some extent in our structures due to the breakdown of the symmetry by a small built-in electric field or asymmetric AlAs inserted layer; the oscillator strength of the transition ehh21 is still much smaller than the transition ehh11. This is exactly what we observed from samples As375 and As364 in Fig. 1. However, the second transition in sample As374 is rather different, with a much stronger transition oscillator strength, which is in agreement with the assignment of the transition ehh22.

Let us now look at how the mobility depends on the position of the AlAs inserted layer. We would like to point out that the three samples were grown under similar conditions and in the same growth run. The three samples were also treated by hydrogen plasma at the same time. Thus the results from the samples are relevant for comparison. The Hall mobility for the three as-grown samples and the H-passivated samples is summarized in Table I. First, the results illustrate that there is no significant change of the Hall mobility among the three samples. Second, the ordering of the Hall mobility among the three samples is different before and after the H treatment. This indicates that the Hall mobility depends essentially on the 2DEG concentration. Since the difference in the as-grown samples and the H-passivated samples is the electron density, the change of the relative Hall mobility is likely related to the change of the electron-phonon scattering, which depends on the electron density.[14,15] However, from our results we do not observe a strong enhancement of the Hall mobility by introducing an AlAs phonon barrier in the well, as has been theoretically predicted.[20] The weak effects of the AlAs inserted layer on the electron mobility may purely be related to our structure geometry and electron concentration in the structures. In order to draw more conclusions, the theoretical calculations of the Hall mobility have to be performed for structures like ours. However, such calculations are beyond the scope of this paper. Nevertheless, our results provide a basis for further theoretical investigations.

Since, on the one hand, the monolayer AlAs inserted layer in modulation doped GaAs/$Al_xGa_{1-x}As$ QW structures strongly influences the optical transition energies, and, on the other hand, the Hall mobility is not significantly changed, the structures presented here may provide a new way to manipulate the properties of modulation doped structures for optical-electronic applications.

In summary, we have presented a detailed investigation of modulation doped GaAs/$Al_xGa_{1-x}As$ quantum-well structures with and without a monolayer of AlAs in the well region. The electronic structures of the modulation doped structures are studied by magnetooptical spectroscopy. dc plasma hydrogen treatments have been used to alter the 2D electron concentration in the well region. The experimental results and theoretical simulations indicate that the monolayer AlAs insertion has a strong influence on the carrier energy levels in modulation doped structures. The effective mass of the 2DEG emission was deduced, and the results do not show any significant variation when an AlAs inserted layer was included in the well region. The Hall mobility was found to be marginally influenced by the position of the inserted layer.

ACKNOWLEDGMENTS

We would like to thank J. Weber for helping us to prepare the dc-hydrogen treated samples. We thank J. Svensson for helping us to do the Hall measurements.

[1] I. V. Kukushkin, K. von Klitzing, K. Ploog, V. E. Kirpichev, and B. N. Sheoel, Phys. Rev. B **40**, 4179 (1989).

[2] Q. X. Zhao, J. P. Bergman, P. O. Holtz, B. Monemar, C. Hallin, M. Sundaram, J. L. Merz, and A. C. Gossard, Semicond. Sci. Technol. **5**, 884 (1990); Phys. Rev. B **43**, 5035 (1991).

[3] Q. X. Zhao, P. O. Holtz, B. Monemar, E. Sörman, W. M. Chen, C. Hallin, M. Sundaram, J. L. Merz, and A. C. Gossard, Phys. Rev. B **46**, 4352 (1992).

[4] J. P. Bergman, Q. X. Zhao, P. O. Holtz, B. Monemar, M. Sundaram, J. L. Merz, and A. C. Gossard, Phys. Rev. B **43**, 4771 (1991).

[5] L. M. Weegels, J. E. M. Haverkort, M. R. Leys, and J. H. Wolter, Phys. Rev. B **46**, 3886 (1992).

[6] W. Chen, M. Fritze, A. V. Nurmikko, M. Hong, and L. L. Chang, Phys. Rev. B **43**, 14 738 (1991).

[7] M. S. Skolnick, J. M. Rorison, K. J. Nash, D. J. Mowbray, P. R. Tapster, S. J. Bass, and A. D. Pitt, Phys. Rev. Lett. **58**, 2130 (1987).

[8] T. Lundström, J. Dalfors, P. O. Holtz, Q. X. Zhao, B. Monemar, G. Landgren, and J. Wallin, Phys. Rev. B **54**, 10 637 (1996).

[9] B. J. F. Lin, Ph.D. thesis, Princeton University, Princeton, NJ (1984).

[10] J. M. Moison, F. Houzay, F. Barthe, and L. Leprince, Appl. Phys. Lett. **64**, 196 (1994).
[11] Q. Xie, A. Madhukar, P. Chen, and N. P. Kobayashi, Phys. Rev. Lett. **75**, 2542 (1995).
[12] V. Calvo, P. Lefebvre, J. Allegre, A. Bellabchara, H. Mathieu, Q. X. Zhao, and N. Magnea, Phys. Rev. B **53**, R16 164 (1996).
[13] Q. X. Zhao, N. Magnea, and M. Willander, J. Phys. C **10**, 1839 (1998).
[14] J. Pozela, V. Juciene, A. Namajunas, and K. Pozela, Phys. Status Solidi B **204**, 238 (1997).
[15] J. Pozela, V. Juciene, A. Namajunas, and K. Pozela, J. Appl. Phys. **81**, 1775 (1997).
[16] Q. X. Zhao, B. O. Fimland, U. Södervall, M. Willander, and E. Selvig, Appl. Phys. Lett. **71**, 2139 (1997).
[17] M. H. Meynadier, J. Orgonasi, C. Delalande, J. A. Brum, G. Bastard, M. Voos, G. Weimann, and W. Schlapp, Phys. Rev. B **34**, 2482 (1986).
[18] C. Delalande, G. Bastard, J. Orgonasi, J. A. Brum, H. W. Liu, M. Voos, G. Weimann, and W. Schlapp, Phys. Rev. Lett. **59**, 2690 (1987).
[19] G. E. Bauer, Surf. Sci. **229**, 374 (1990).
[20] K. Pozela (private communication).